Anal. Chem. **2005,** *77,* 1177−1182

Moving beyond Traditional UV−Visible Absorption Detection: Cavity Ring-Down Spectroscopy for HPLC

Kate L. Bechtel,[†,‡] Richard N. Zare,[*,†] Alexander A. Kachanov,[§] Steve S. Sanders,[§] and Barbara A. Paldus[§]

Department of Chemistry, Stanford University, Stanford, California 94305-5080, and Picarro, Inc., 480 Oakmead Parkway, Sunnyvale, California 94085

We describe the use of liquid-phase continuous-wave cavity ring-down spectroscopy for the detection of an HPLC separation. This technique builds on earlier work by Snyder and Zare using pulsed laser sources and improves upon commercially available UV−visible detectors by a factor of up to 50. The system employs a compact doubled-diode single-mode continuous-wave laser operating at 488 nm and a previously described Brewster's-angle flow cell. Ring-down time constants as long as 5.8 μs were observed with liquid samples in a 0.3-mm path length cell. The baseline noise during an HPLC separation was only 2×10^{-7} absorbance units (AU) peak to peak, as compared to 1×10^{-5} AU for a state-of-the-art commercial UV−visible detector.

Although traditional UV−visible absorption spectroscopy is well established for the detection of liquid-phase analytes, cavity-enhanced techniques have recently emerged as a high-sensitivity alternative. Of the various implementations found in the literature, cavity ring-down spectroscopy (CRDS) appears to have the most potential. CRDS is an absorption technique established by O'Keefe and Deacon in 1988 and is inherently multipass and insensitive to incident light intensity fluctuations.[1−3] In the simplest CRDS system, a laser pulse is incident on an optical cavity formed from two highly reflective mirrors facing each other. A small fraction of this light, approaching $1 - R$, where R is the mirror reflectivity, passes through the first mirror and proceeds to bounce back and forth between the mirrors, losing a corresponding fraction of its intensity on each bounce. A photodetector placed behind the second mirror records the decay of light intensity exiting the cavity. This decay, referred to as the "ring-down profile", is exponential and possesses a characteristic time constant, τ. The ring-down time constant is inversely proportional to all optical losses within the cavity:

$$\tau = \frac{L}{c[(1 - R) + \delta_c + \alpha l]}. \quad (1)$$

In this equation, L is the distance between the cavity mirrors, c is the speed of light in the cavity medium, δ_c includes cavity losses other than those arising from the mirrors, i.e., those caused by optics placed within the cavity and absorption and scattering of light by the cavity medium, and αl is the absorption loss of any analytes that may be present. For simplicity in expressing this equation, the index of refraction of the cavity medium is taken to be unity though this assumption is not always true, particularly if the cavity contains a long optical path length of liquid sample. The sample path length, l, is equal to the cavity length, L, for most gas-phase experiments. However, in our experiments, the liquid-phase analyte is contained within a cell inside the cavity and therefore the sample path length and mirror separation differ. The absorption coefficient, α, may be found by recording the ring-down time, τ_o, without the analyte in the cavity, and the ring-down time, τ, with the analyte in the cavity and using the relation

$$\alpha = \frac{L}{cl}\left(\frac{1}{\tau} - \frac{1}{\tau_o}\right) \quad (2)$$

For comparison with HPLC measurements, the absorption coefficient is related to Beer's law absorbance, A, by the equation

$$A = \epsilon l C = \frac{\alpha l}{2.303} = \frac{L}{2.303c}\left(\frac{1}{\tau} - \frac{1}{\tau_o}\right) \quad (3)$$

where ϵ is the molar absorptivity, C is the analyte concentration, and 2.303 is the conversion factor between natural log and log base 10.

* To whom correspondence should be addressed. Fax: (650) 723-9262. E-mail: zare@stanford.edu.

† Stanford University.

‡ Present address: GR Harrison Spectroscopy Laboratory, Massachusetts Institute of Technology, Cambridge, MA 02139.

§ Picarro, Inc.

(1) O'Keefe, A.; Deacon, D. A. G. *Rev. Sci. Instrum.* **1988**, *59*, 2544−2551.

(2) O'Keefe, A.; Scherer, J. J.; Cooksy, A. L.; Sheeks, R.; Heath, J.; Saykally, R. J. *Chem. Phys. Lett.* **1990**, *172*, 215−218.

(3) Zalicki, P.; Zare, R. N. *J. Chem. Phys.* **1995**, *102*, 2708−2717.

10.1021/ac048444r CCC: $30.25
Published on Web 01/21/2005

The minimum detectable absorption coefficient per pass is given by[4]

$$\alpha_{min} = \sqrt{2}\frac{L(\sigma_\tau/\bar{\tau}_o)}{lc\bar{\tau}_o} \quad (4)$$

where σ_τ is the standard deviation of the mean value of the ring-down time, $\bar{\tau}_o$, without the analyte present. The value $\sigma_\tau/\bar{\tau}_o$ is a measure of the shot-to-shot variation in the ring-down time constant. From this equation it is clear that in order to obtain a low detection limit, this shot-to-shot variation must be minimized and $\bar{\tau}_o$ maximized.

CRDS may be performed with both pulsed and continuous-wave laser sources. Pulsed-laser CRDS, though simpler to implement experimentally, often presents difficulties in achieving low shot-to-shot variations owing to the excitation of higher order transverse modes. Higher order modes have elevated optical losses in the ring-down cavity, and the distribution of energy within these modes can randomly vary from pulse to pulse. As a result, the shot-to-shot variation in the ring-down time constant can be relatively large.[5] In continuous-wave CRDS (cw-CRDS), narrow line width lasers permit the excitation of only a single transverse mode (TEM_{00}),[6] thereby greatly improving the shot-to-shot performance. By using appropriate mode matching, the shot-to-shot variation can be further reduced to the digitization limit of the ring-down decay waveforms.[7] Additionally, cw-CRDS systems allow the laser and the cavity to be locked together such that the same mode is repeatedly excited, leading to extreme sensitivities on the order of 1×10^{-12} $cm^{-1}/Hz^{-1/2}$.[8]

Liquid-Phase CRDS. Unlike gaseous samples, liquid samples create an index step within the optical cavity, precluding more common cavity designs. Furthermore, unlike solids, liquid samples require containment. As a result of these complications, the extension of CRDS to liquid samples only started appearing in the literature a decade after the inception of this technique. Since then, many different approaches have been developed, with varying degrees of success.

The first of these approaches, evanescent-wave cavity ring-down spectroscopy (EW-CRDS), was proposed by Pipino et al. in 1997.[9,10] EW-CRDS relies on the production of an evanescent field at a total internal reflection interface between an optical medium and a sample in order to probe a surface layer of the sample. The first configuration placed a Pellin−Broca prism inside an L-shaped ring-down cavity, thereby producing one surface in the prism having total internal reflection. The evanescent wave produced by this internal reflection has been used to probe liquid samples. Other embodiments of EW-CRDS include multifaceted polygonal cavities,[11,12] Dove prisms,[13] and fiber loops.

The first uses of fiber ring-down cavities appear in the literature in 2002, although they were suggested earlier.[14,15] The high-reflectivity mirrors on each end of the fiber can be either dielectrically coated, as in a traditional ring-down cavity design, or can consist of fiber Bragg gratings.[16] Fiber-based CRDS has been applied to detection in liquid samples via a fiber loop cavity wherein the liquid sample replaces the index matching fluid in the gap between fibers at the connector splice.[17]

More direct approaches to measuring liquid samples also appeared in 2002. Hallock, Berman, and Zare[18] demonstrated direct detection by using a traditional CRDS setup in which the linear cavity was filled with a liquid sample of copper(II) acetate (620−670 nm) in acetonitrile solution. Alternatively, the placing of a liquid sample at Brewster's angle in a ring-down cavity had been proposed earlier.[19] Xie et al.[20] first demonstrated this idea experimentally by inserting a UV−visible cuvette oriented at Brewster's angle into the ring-down cavity. This approach was limited to samples having an index of refraction of 1.46. Such samples are not common, and therefore, this approach could not be widely applied. However, a similar approach was utilized by Alexander[21] for the study of reaction kinetics of nitrate radicals with terpenes in solution. Snyder and Zare[22] resolved these limitations by designing a flow cell with wedged angles that minimize optical losses for any given index of refraction medium by allowing *p*-polarized light to refract through all cell interfaces (air/fused silica/liquid/fused silica/air) at Brewster's angle. Brewster's angle, defined as $\tan^{-1} n_t/n_i$, where n_i is the refractive index of the incident medium and n_t is the refractive index of the transmitted medium, is the angle at which light polarized parallel to the plane of incidence has no reflection loss. Such a flow cell was coupled to the output of an HPLC separation, enabling the first detection of separated analytes by their absorption properties using CRDS.

The experimental setup for that system utilized a pulsed laser source at 470 nm and detected a series of anthraquinones. Ring-down time constants with the Brewster's-angle flow cell, having an interior optical path length of 0.3 mm, were up to 2.5 μs in a 1-m cavity. The peak-to-peak baseline noise level of this system was 1.0×10^{-5} absorbance units (AU), rivaling the best available commercial UV−visible detectors. The CRDS detector performance, while notable, was limited in this case because of the nature of the light source; excitation of multiple cavity modes resulted in a 1% shot-to-shot variation in the ring-down time constant.

(4) Romanini, D.; Lehmann, K. K. *J. Chem Phys.* **1993**, *99*, 6287−6301.
(5) Hodges, J. T.; Looney, J. P.; van Zee, R. D. *J. Chem. Phys.* **1996**, *105*, 10278−10288.
(6) Romanini, D.; Kachanov, A. A.; Sadeghi, N.; Stoeckel, F. *Chem. Phys. Lett.* **1997**, *264*, 316−322.
(7) Crosson, E. R.; Ricci, K. N.; Richman, B. A.; Chilese, F. C.; Owano, T. G.; Provencal, R. A.; Todd, M. W.; Glasser, J.; Kachanov, A. A.; Paldus, B. A.; Spence, T. G.; Zare, R. N. *Anal. Chem.* **2002**, *74*, 2003−2007.
(8) Spence, T. G.; Harb, C. C.; Paldus, B. A.; Zare, R. N.; Willke, B.; Byer, R. L. *Rev. Sci. Instrum.* **2000**, *71*, 347−353.
(9) Pipino, A. C. R.; Hudgens, J. W.; Huie, R. E. *Rev. Sci. Instrum.* **1997**, *68*, 2978−2989.
(10) Pipino, A. C. R.; Hudgens, J. W.; Huie, R. E. *Chem. Phys. Lett.* **1997**, *280*, 104−112.
(11) Pipino, A. C. R. *Phys. Rev. Lett.* **1999**, *83*, 3093−3096.
(12) Pipino, A. C. R. *Appl. Opt.* **2000**, *39*, 1449−1453.
(13) Shaw, A. M.; Hannon, T. E.; Li, F.; Zare, R. N. *J. Phys. Chem. B* **2003**, *107*, 7070−7075.
(14) von Lerber, T.; Sigrist, M. W. *Appl. Opt.* **2002**, *41*, 3567−3575.
(15) European Patent EP00121314.9, 2002.
(16) Gupta, M.; Hong, J.; O'Keefe, A. *Opt. Lett.* **2002**, *27*, 1878−1880.
(17) Brown, R. S.; Kozin, I.; Tong, Z.; Oleschuk, R. D.; Loock, H. P. *J. Chem. Phys.* **2002**, *117*, 10444−10447.
(18) Hallock, A. J.; Berman, E. S. F.; Zare, R. N. *Anal. Chem.* **2002**, *74*, 1741−1743.
(19) Paldus, B. A.; Harb, C.; Zare, R. N.; Meijer, G. U.S. Patent 6452680, 2002.
(20) Xu, S.; Sha, G.; Xie, J. *Rev. Sci. Instrum.* **2002**, *73*, 255−258.
(21) Alexander, A. J. *Chem. Phys. Lett.* **2004**, *393*, 138−142.
(22) Snyder, K. L.; Zare, R. N. *Anal. Chem.* **2003**, *75*, 3086−3091.

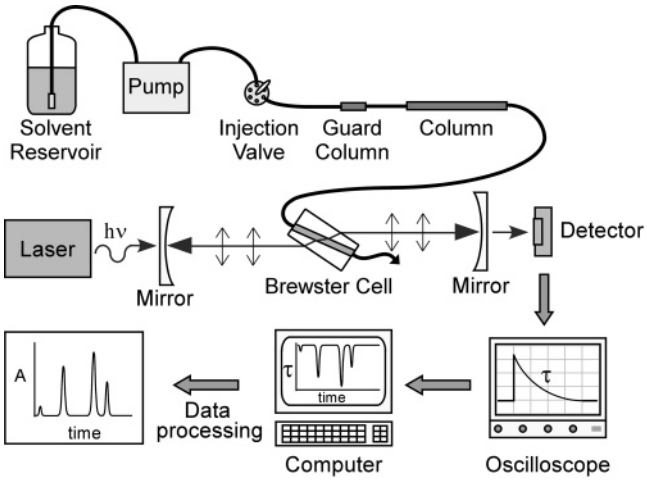

Figure 1. Illustration of the HPLC−CRDS operating principle and data analysis. Bands of analytes that are separated by the column pass through the Brewster's-angle flow cell and are detected by CRDS. The ring-down time constant, τ, is plotted as a function of time to reveal the absorbing analytes. The τ values can be converted into absorbance units, yielding a standard chromatogram (see also Figure 4).

Table 1. Structures of Anthraquinones

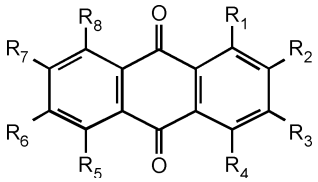

	name	R_1	R_2	R_3	R_4	R_5	R_6	R_7	R_8
1	alizarin	OH	OH	H	H	H	H	H	H
2	purpurin	OH	OH	H	OH	H	H	H	H
3	quinalizarin	OH	OH	H	H	OH	H	H	OH
4	emodin	OH	H	OH	H	H	CH_3	H	OH
5	quinizarin	OH	H	H	OH	H	H	H	H

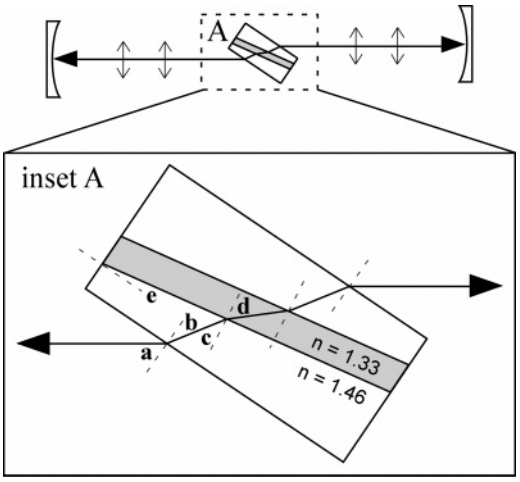

Figure 2. Schematic diagram of the Brewster's-angle flow cell inside a ring-down cavity. The vertical double arrows indicate the light is polarized parallel to the plane of incidence of the cell. The inset shows an expanded view of the cell. With a material index of 1.46 for fused silica and a liquid index of 1.33 for water, the optimal wedge angle, *e*, is 7.9°. With this configuration the cell should be tilted so that the angle of light incidence, *a*, is 55.6°. The light refracts through the cell, hitting each surface at the appropriate angle for minimum reflection. These Brewster's angles are $b = 34.4°$, $c = 42.3°$, and $d = 47.7°$.

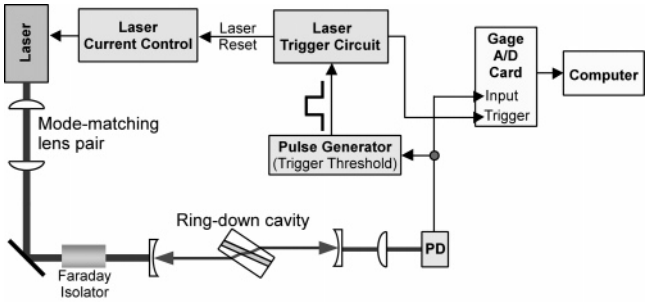

Figure 3. Experimental diagram for liquid-phase continuous-wave cavity ring-down spectroscopy with laser current switching.

The minimum detectable absorbance of the liquid-phase CRDS detector can be improved through the use of a single-mode, continuous-wave laser source. The narrow laser line width enables excitation of a single cavity mode and high suppression of higher order cavity modes. As a result, the shot-to-shot variation in the ring-down time constant can be reduced to 0.04%. Through improved cell characterization, ring-down time constants with the same flow cell and cavity length can be improved to nearly 6 μs. This paper presents the first results of cw-CRDS applied to liquid samples using the previously developed Brewster's-angle cell. We also present a comparison between cw-CRDS detection for an HPLC separation versus a state-of-the-art commercial UV−visible detector.

EXPERIMENTAL SECTION

Figure 1 illustrates the basic operating principle of cavity ring-down spectroscopy as a detector for HPLC. In this figure, the output of an HPLC column is connected to the Brewster's-angle flow cell located inside the ring-down cavity. Appropriately polarized light, indicated by parallel arrows, is directed into the cavity and the value of the ring-down time constant, τ, is recorded versus time. As the analyte bands pass through the flow cell, the value of τ will change in relation to the magnitude of light absorption by the analyte. The resulting chromatogram can thus be easily converted into standard Beer's law absorbance values versus time using eq 3 and directly compared with the results of a commercial HPLC instrument with UV−visible detection.

HPLC. Chromatography was performed with a Shimadzu LC-10ADvp pump with a flow rate of 1.0 mL/min., a Valco Cheminert or a Rheodyne six-port injection valve equipped with a 20-μL sample loop, a Shimadzu CTO-10ACvp column oven (22 °C), and an Agilent Zorbax Eclipse XDB-C18 guard column and analytical column. The end-capped C_{18} column contains 5-μm particles and has dimensions of 150 mm × 4.6 mm i.d. The separation is carried out using an isocratic mobile phase of methanol/5% acetic acid in water (80:20 v/v) with a pH of 3.6. Spectroscopic-grade methanol and ultrapure water (18.2 MΩ·cm Millipore Milli-Q) are used in the mobile phase. A Shimadzu SPD-10AVvp detector and an SCL-10Avp controller were used for the UV−visible comparison.

Analytes. Alizarin (1,2-dihydroxyanthraquinone), purpurin (1,2,4-trihydroxyanthraquinone), quinalizarin (1,2,5,8-tetrahydroxyanthraquinone), emodin (6-methyl-1,3,8-trihydroxyanthraquinone), and quinizarin (1,4-dihydroxyanthraquinone) were purchased from

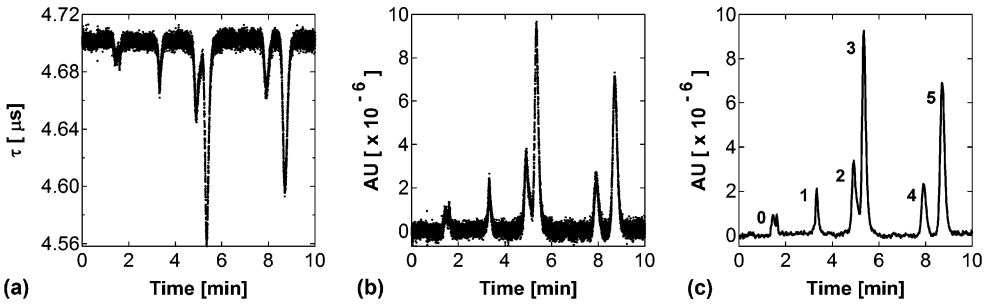

Figure 4. Conversion from individual ring-down time measurements to a standard chromatogram. Labeled peaks: 0, solvent front; 1, alizarin; 2, purpurin; 3, quinalizarin; 4, emodin; and 5, quinizarin. The concentration of each analyte is 0.3 μM. (a) Raw τ data obtained by fitting individual ring-down waveforms. (b) The raw τ data converted into absorbance units. **(c)** The data from (b) averaged over 1 s to obtain the final chromatogram.

Sigma-Aldrich (St. Louis, MO) and used without further purification. These molecules are members of the anthraquinone family, and their structures are shown in Table 1.

Brewster's-Angle Flow Cell. The cell used in these experiments is the same cell used in the prior HPLC−CRDS experiments with a pulsed laser source. The cell was constructed by Hellma Cells, Inc., (Plainview, NY) according to our instructions. It is composed of two well-polished UV-grade fused-silica wedges that are fused at high temperature. The optical path length is 0.3 mm, taking into consideration the propagation of light at Brewster's angle. The total cell volume is 10 μL, though the illuminated volume is only 0.5 μL. A schematic of the cell angles is shown in Figure 2.

Four solvents—methanol, water, acetonitrile, and acetone—with indices of refraction ranging from approximately 1.32 to 1.36, were placed individually in the Brewster's-angle cell. The ring-down times for all four solvents were in the range of 5.2−5.4 μs, indicating that the variation of solvent absorption or the small refractive index differences do not significantly affect the performance of the HPLC measurements in an isocratic mobile phase. However calibration will be necessary for gradient elutions. Additionally, very clean, degassed solvents are required for the mobile phase as substantial decreases in ring-down time were observed when microscopic bubbles entered the cell (noticed by increased scattering of the blue light from the inner part of the cell) or when the solvent was not sufficiently pure.

The ring-down time was highly dependent on cell cleanliness and air quality. The outer surface of the cell was cleaned every few days (or whenever the ring-down time was less than 4 μs) with both spectroscopic-grade methanol and acetone. The cavity was continuously purged with dry nitrogen to decrease noise attributed to dust and particulates.

cw-CRDS System. The continuous-wave cavity ring-down system designed for these experiments is illustrated in Figure 3. A Picarro Cyan 488-nm cw single-mode laser was used as the light source and appropriately mode-matched to the ring-down cavity. Its circuitry was modified in order to permit laser current shutdown by an external trigger signal. The following automated sequence was used to acquire ring-down profiles: (i) The laser current is turned on to enable the laser. (ii) During startup, the laser emission frequency changes owing to thermal effects on the laser medium. (iii) As the frequency sweeps, it coincides with a cavity mode resulting in energy buildup inside the cavity. (iv) This radiation buildup is detected by a photodiode placed at the cavity output. (v) When the photodiode signal reaches a threshold value, a trigger signal is produced by the pulse generator and sent to the laser controller to shut off the current. The laser intensity drops from 90 to 10% of its maximum value in 0.48 μs and is completely shut off in less than 1 μs. (vi) Simultaneously, a trigger signal is sent to the data acquisition system to record the decay of light intensity (ring-down waveform) observed by the photodiode. (vii) The laser shutoff time was set to be 100 μs, which is ~10 times longer than the maximum expected ring-down time to ensure the entire ring-down and sufficient baseline were recorded before injecting light into the cavity again.

This process is repeated at a rate of 20−40 Hz. The data acquisition rate is limited by the laser startup dynamics.

Data Analysis. The output of the photodetector monitoring the ring-down was sent to an A/D card (GageScope CS1250, 12-bit, 50 Ms/s) and processed on a PC. Ring-down time constants were abstracted from each ring-down waveform using a fast fitting algorithm developed by Halmer et al.[23] Figure 4a shows the raw measured values of the τ data plotted as a function of time. The scattering of data points in the baseline region correspond to a shot-to-shot variation of 0.05%. These data were converted into absorbance units by use of eq 3, where τ_0 was determined by a least-squares fit of the baseline (Figure 4b). The data points were then averaged over 1 s to obtain a chromatogram comparable to that derived from a UV−visible detector (Figure 4c).

RESULTS AND DISCUSSION

Peak Reproducibility. A 22 μM sample of alizarin was repeatedly injected onto the HPLC column and detected by cw-CRDS to obtain a measure of peak reproducibility. The raw data of τ versus time were converted to absorbance units and overlaid. The overall shape of the alizarin peak was quite reproducible over the seven runs (Figure 5), and the peak height reproducibility was 0.11%.

HPLC Calibration. HPLC calibration curves for the heights and areas of each of the five compounds used in these experiments were measured. The peak heights and areas were determined using the program PeakFit (SYSTAT Software). Each curve was linear, with R^2 values exceeding 0.9999 with the exception of purpurin, whose R^2 value was 0.995 owing to the proximity of an impurity peak that made difficult the accurate determination of purpurin peak height and area. The concentration ranges for each compound were as follows: alizarin, 0.3−55 μM; purpurin, 0.07−

(23) Halmer, D.; von Basum, G.; Hering, P.; Murtz, M. *Rev. Sci. Instrum.* **2004**, *75*, 2187−2191.

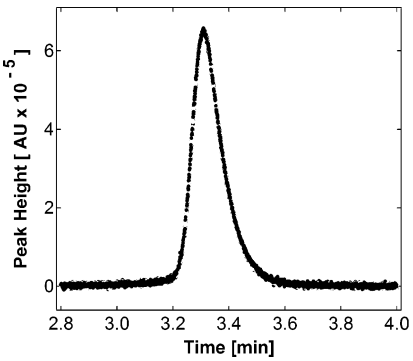

Figure 5. Seven overlaid traces of 22 μM alizarin. The raw data are converted to AU directly from individual measurements of τ and are not smoothed or filtered.

25 μM; quinalizarin, 0.03−7 μM; emodin, 0.1−30 μM; quinizarin, 0.1−10 μM.

The linear dynamic range of the instrument was estimated to be 2.5 orders of magnitude. The maximum value of absorbance that the system could measure was just over 2.5×10^{-4} AU, which greatly limits the utility of the instrument. At higher sample concentrations, the sample absorbs most of the light, which results in low signal levels from the fixed-gain photodetector at the cavity output. If the signal level is below the predetermined threshold, the data acquisition system will not be triggered. The photodiode signal is used as the basis for a trigger because the coupling of light into the cavity is dependent on the laser frequency overlapping a cavity mode, which is an otherwise unpredictable event. If the data acquisition system were to be triggered without a substantial buildup of light within the cavity, the ring-down signal would be too low in intensity to obtain its decay time without errors. A possible solution to the problem of low light levels would be to control electronically the avalanche photodiode gain such that it would increase as an analyte passes through the Brewster's-angle cell. In practice, ring-down times as short as a few hundred nanoseconds should be measurable, which would correspond to absorbance values on the order of 10^{-3} AU. This approach could increase the linear dynamic range by an order of magnitude.

HPLC Measurements. Figure 6 displays the results of HPLC separations detected both by cw-CRDS and by a representative high-quality UV−visible detector (Shimadzu SPD-10AVvp). The path length of the prototype Brewster's-angle flow cell is 0.3 mm compared to the UV−visible path length of 10 mm. Thus, the concentrations of the samples were adjusted accordingly to compare equivalent absorbance values. The result of this comparison is shown in Figure 6a and b. Furthermore, the cw-CRDS system can detect the same low 100 nM concentration as the UV−visible detector though the latter detector's path length is 33 times longer, as seen in Figure 6c and d. The entirety of the cw-CRDS trace (Figure 6c) would be well within the peak-to-peak noise of any commercial UV−visible detector. The peak-to-peak baseline noise was only 2×10^{-7} AU, and the rms noise was 3.4×10^{-8} AU.

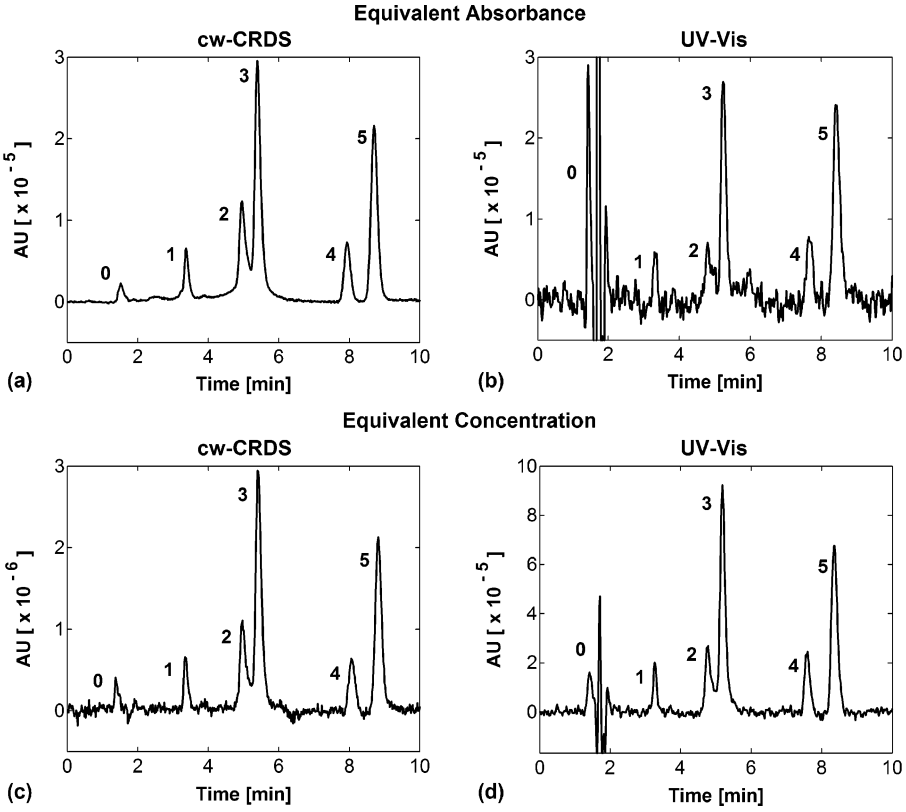

Figure 6. Comparison of chromatograms obtained by the cw-CRDS detector and by a state-of-the-art commercial UV−visible detector (Shimadzu SPD10AVvp). Labeled peaks: 0, solvent front; 1, alizarin; 2, purpurin; 3, quinalizarin; 4, emodin; and 5, quinizarin. (a) cw-CRDS detection with 0.3-mm path length and 1 μM concentrations. The small peaks at approximately 2.5 and 4 min are impurities that are easily measured at higher concentrations. (b) UV−visible detection with 10-mm path length and 0.03 μM concentrations. Traces a and b compare equivalent absorbance values. (c) cw-CRDS detection with 0.3-mm path length and 0.1 μM concentrations. (d) UV−visible detection with 10-mm path length and 0.1 μM concentrations. Traces c and d compare equivalent concentrations though absolute absorbance values differ by a factor of 33 owing to the difference in path lengths.

CONCLUDING REMARKS

The application of continuous-wave CRDS to liquid-phase detection offers a significant improvement over traditional UV−visible absorption spectroscopy and can provide a new tool for analytical chemists. These results clearly illustrate the potential of liquid-phase cw-CRDS and its use as an absorption detector for HPLC measurements. Further room for improvement exists. For example, a longer path length cell (1.5 mm) with the same volume is in development. Preliminary results suggest it can provide similar minimum detectable absorbances with a 5-fold reduction in the concentration detection limit. Another major improvement to the system would involve a reduction in its operating wavelength. Currently, absorption at 488 nm requires the analyte to be colored. Although this wavelength may be useful to pharmaceutical companies detecting yellowing of their compounds or for the detection of certain vitamins and pigments, widespread applications would be better served in the ultraviolet. Unfortunately, semiconductor lasers in the region of interest (250−280 nm) with the required specifications are not available at this time. Additionally, mirror coating technology has not yet provided high-reflectivity mirrors in this wavelength range. However, with the current rate of technological improvements, an ultraviolet cw-CRDS system should be realized within the next few years. Finally, challenges still remain in the extension of the dynamic range and integration of this technique with existing HPLC systems.

ACKNOWLEDGMENT

We thank Dr. Yutaka Kohno, Shimadzu Corp., for the generous loan of the Shimadzu HPLC instrument. K.L.B. is grateful for a Schering Plough/The Leadership Alliance fellowship. This material is based upon work supported by the National Science Foundation under Grant DMI-0320431.

Received for review October 20, 2004. Accepted December 4, 2004.

AC048444R